

# A Novel Comparative Study: Synthesis, Characterization, and Thermal Degradation Kinetics of a Copolymer and Its Composites with Activated Charcoal

Punam G. Gupta<sup>1</sup>, R. H. Gupta<sup>2</sup>, W. B. Gurnule<sup>1</sup>

Department of Chemistry, Kamla Nehru Mahavidyalaya, Sakkardara, Nagpur, India<sup>1</sup>

Department of Chemistry, K. Z. S. Science College, Kalmeshwar, Nagpur, India<sup>2</sup>

wbgurnule@yahoo.co.in<sup>1</sup>

**Abstract:** A novel composite was prepared by using a copolymer involving 2-amino 6-nitrobenzothiazole– formaldehyde copolymer and activated charcoal. Physicochemical analysis, elemental and spectrum analysis were used to characterize the produced copolymer and its composite. SEM and thermogravimetric analysis (TGA) was used to study the surface morphology and thermal stability of the copolymer and its composites, respectively. The composite produced better results, which could be attributed to the particle size, porous nature, and increased surface area. The thermal stability of the copolymer and its composite had been improved. The thermodynamic kinetic parameters activation energy, free energy, apparent entropy, frequency factor, and entropy change were also estimated from TG data using the Sharp-Wentworth and Freeman-Carroll methods, and the findings were found to be similar. First-order kinetics were used to decompose the copolymer and its composite. The copolymer and its composite decomposed using first-order kinetics.

**Keywords:** Composites; Charcoal; Activation Energy; Thermogravimetric; Free Energy.

## I. INTRODUCTION

Polymeric materials have worldwide uses in polymer science and innovation have been growing quickly and pulled in much consideration towards the polymer researchers. Polymers have been discovered to be helpful applications as adhesive [1], high-temperature, fire-proofing coating materials [2], semiconductors, catalysts, and ion-exchange resins[3]. Terpolymer has been synthesized by the various researcher by different polymerization methods to examine its advanced applications. In recent year, terpolymer was synthesized by using monomers like 2,4-dihydroxyacetophenone-dithioamide-formaldehyde[4]8-hydroxyquinoline-guanidine-formaldehyde[5], resorcinol-urea-formaldehyde[6], salicylic acid-thiourea-trioxane[7], 2-hydroxyacetophenone-oxamide-formaldehyde [8], 2,4-dihydroxypropiofenone-biuret-formaldehyde [9], 2,2'-dihydroxybiphenyl-urea-formaldehyde [10]. Several researchers have synthesized and characterized various copolymers to study their thermal stability. Further, various polymers and itscomposite have also been studied for the thermal behavior and decomposition kinetics.

Thermal analysis is an important property of polymer as it gives information about thermal stability and processability of the synthesized polymer [11] also it is used to determine the structure and properties of materials [12]. To incorporate polymers having various practical applications, there is a need to explore the impact of heat on the polymers to set up their thermal stability. The thermal behavior study of terpolymers gives the data of degradation of various groups produced in different temperatures and environments[13] The study reported that the TGA technique can be applied to 2,4-dihydroxybenzoic acid –melamine-formaldehyde copolymer to evaluate the activation energy by nonisothermalthermogravimetric methods [14].The thermal stability of copolymer derived from 2-Hydroxyl, 4-methoxybenzophenone, 1,5- diamionaphthalene, and formaldehydewere determined using Sharp-Wentworth and Freeman-Carroll methods [15]. Terpolymer resin derived from salicylaldehyde, ethylenediamine and formaldehyde



### 2.3. Preparation of Copolymer composites with activated charcoal

The novel copolymer/activated charcoal composite was prepared by polymer (1.0 g) and activated charcoal (2.0 g) in 1:2 ratios. The copolymer dissolved in 25 ml DMSO was taken in a 100ml beaker and activated charcoal was added into it and the mixture was subjected to ultrasonication for 3 h with constant stirring at room temperature. After the specific time, the black color composite was obtained and separated, washed with ethanol and acetone to remove the impurities, the composite was filtered and dried at 70°C for 24 h.

### 2.4. Instrumentation

An ElementerVario EL III (Germany) elemental analyzer was used to micro analyze the copolymer for C, H, and N. On a Bruker Alpha-E FTIR spectrophotometer at the RUSA Centre for Bio-Actives and Natural Products, Rashtrasant Tukadoji Maharaj Nagpur University, Nagpur, an infrared spectrum of the copolymer and its composite with activated charcoal was recorded in the range 4000 to 400 cm<sup>-1</sup>. Shivaji Science College, Nagpur, employed a Shimadzu automatic recording double beam spectrophotometer UV-1800 to record electron absorption spectra of the copolymer and its composite in the 200 to 800 nm range in DMSO solvent. At the STIC, Cochin, and SAIF, Dharwad University, the scanning electron micrograph of the copolymer and its composites was scanned and magnified using a scanning electron microscope respectively.

### 2.5. Thermogravimetric Analysis

The thermal degradation kinetics of copolymer and copolymer/activated charcoal composite was analyzed from RUSA Centre for Bio-Actives and Natural Products, Rashtrasant Tukadoji Maharaj Nagpur University, Nagpur with a heating rate of 20°C min<sup>-1</sup>. Thermogravimetric data was used to calculate the thermal activation energies (E<sub>a</sub>), order of reaction (n), entropy change (ΔS), apparent entropy change (S\*), free energy change (ΔF), and frequency factor (Z).

#### Theoretical Considerations

The TG curves were created using the analytical procedures outlined by Freeman-Carroll[19], and Sharp-Wentworth[20] to provide additional information about the degradation mechanism of the examined copolymer and its composite.

#### Sharp-Wentworth Method:

Using the equation derived by Sharp and Wentworth,

$$\log[(dc/dT)/(1-c)] = \log(A/\beta) - [E_a/2.303R] \cdot 1/T \dots \dots \dots (1)$$

Where, dc/dT = rate of change of fraction of weight with change in temperature

β = linear heating rate dT/dt.

By plotting the graph between (logdc/dt)/(1-c) vs 1/T obtained the straight line which gives activation energy (E<sub>a</sub>) calculated from its slope.

Where, β is the conversion at time t,

R is the gas constant (8.314 J mol<sup>-1</sup> K<sup>-1</sup>),

T is the absolute temperature.

#### Freeman-Carroll Method:

Freeman and Carroll's straight-line equation, which has the following form:

$$[\Delta \log(dw/dt)]/\Delta \log W_r = (-E/2.303R) \cdot \Delta(1/T)/\Delta \log W_r + n \dots \dots \dots (2)$$

Where, dw/dt = rate of change of mass with time.

W<sub>r</sub> = W<sub>c</sub> - W

W<sub>c</sub> = weight loss after the reaction.

W = fraction of weight loss at time t.

$E_a$  = activation energy

$n$  = order of reaction.

The plot between the terms  $[\Delta \log (dw/dt)] / \Delta \log W_r V_s \Delta (1/T) / \Delta \log W_r$  gives a straight line and from the value of the slope, we obtained energy of activation ( $E_a$ ) and intercept on Y-axis as the order of reaction ( $n$ ). The change in entropy ( $\Delta S$ ), free energy change ( $\Delta F$ ), frequency factor ( $Z$ ), apparent entropy ( $S^*$ ) can also be calculated by further calculations[21][22][23].

### III. RESULTS AND DISCUSSION

#### 3.1 Physicochemical and Elemental Analysis

It was discovered that the newly synthesized BOF-II copolymer was yellow. The newly synthesized copolymer was found to be soluble in solvents such as DMF, DMSO, THF, and conc.  $H_2SO_4$  while insoluble in almost all inorganic and organic solvents. The copolymer's yield was discovered to be 86%. The BOF-charcoal composites were found to be soluble in DMSO when dispersed in it. The copolymer's hydrogen, carbon, sulphur, and nitrogen content were studied. As a result of elemental analysis, the copolymer's empirical formula and empirical formula weight have been assigned and are shown in Table 1.

**Table 1:** The Physicochemical and Analytical Data of the BOF-II Copolymer

Copolymer	The empirical formula of repeating unit	Empirical formula weight	%C Found (Cal.)	% H Found (Cal.)	% N Found (Cal.)	% S Found (Cal.)
BOF-II	$C_{19}H_{14}N_8O_6S_2$	514	44.93(45.50)	2.79(3.05)	21.01(21.22)	10.97(11.33)

#### 3.2 UV-Visible Spectral Analysis

The UV-visible spectra of the BOF-II copolymer and its composites were recorded in DMSO solvent in the 200-800nm region, as shown in Fig. Two distinctive bands at 269 nm and 360 nm are present in the newly produced BOF-II copolymer, which was depicted in Fig. 2(a). The absorption bands have varied intensities at their observed positions. Because of the allowed transition ( $\pi \rightarrow \pi^*$ ), the band obtained at 269 nm is less intense. Due to the presence of a benzothiazole ring, the allowed  $\pi \rightarrow \pi^*$  transition is obtained which easily achieves coplanarity and shoulder merging (loss of fine structure), as well as chromophore groups such as  $C=O$ ,  $>C=C$ ,  $>C=N$ , and  $-NO_2$  groups in conjugation with an aromatic nucleus (benzothiazole ring). And the more intense band at 360 nm could be due to the ( $n \rightarrow \pi^*$ ) transition, which indicates the presence of  $-NH$  auxochrome. As a result, the presence of aromatic nuclei and  $-NH$  groups is confirmed by the  $\pi \rightarrow \pi^*$  and  $n \rightarrow \pi^*$  transition respectively. A combination of conjugation (due to the chromophore) and  $-NH$  groups (auxochrome) may be responsible for bathochromic shifts (a shift towards longer wavelength) from the basic value, i.e. 240 and 310 nm. The presence of  $-NH$  groups (auxochromes) causes hyperchromic shift ( $\epsilon_{max}$  higher values).

The UV-Vis spectra of the composite show two absorption bands at 250 nm and 330 nm, as illustrated in Fig. 2(b). The presence of an aromatic ring (i.e. benzothiazole ring) in the composite is clearly shown by the absorption band at 250 nm, which could be attributable to  $\pi \rightarrow \pi^*$  transition. The band at 330 nm reveals the presence of the  $-NH$  group in the composite and is assigned to the  $n \rightarrow \pi^*$  transition. The shifting of bands, as seen in Fig.2, can confirm the creation of composites. And, as a result of the findings, composites' absorption decreased when compared to copolymers. As a result of the above considerations, the formation of composites was confirmed[24][25].

#### 3.3 FTIR Spectral Analysis

FTIR spectra in Fig. 3 confirmed the chemical structure of the produced copolymer and their composite including various functional groups. IR spectra revealed that the copolymers and its composite have a nearly identical spectra pattern. The FTIR spectra of the newly synthesized BOF-II copolymers are shown in Fig. 3(a). Previous work has been used to determine the band frequencies and designated groups of the copolymer[26][27]. The band that emerged at  $3607\text{cm}^{-1}$  is caused by the  $-NH$  asymmetric and symmetric vibrations. The emergence of a band at  $1505\text{cm}^{-1}$  is caused by the  $-NO_2$  group of the benzothiazole ring stretching mode. The band at  $1532\text{cm}^{-1}$  is caused by a  $C=O$

stretching vibration. The copolymer's 2,6,8-trisubstituted benzothiazole ring generates sharp and medium absorption bands in the 1195-916cm<sup>-1</sup> range. The -CH<sub>2</sub> asymmetrical and symmetrical vibrations in the BOF-II copolymers were confirmed by the absorption band formed by 3006cm<sup>-1</sup>. The aromatic ring's -CH stretching vibrations have been assigned a band at 2908cm<sup>-1</sup>. The band occurring at 1442 cm<sup>-1</sup> suggests the -CH<sub>2</sub> bending vibration in the N-CH<sub>2</sub>-N Bridge in the copolymer. The band at 786cm<sup>-1</sup> verifies the presence of the C-S-C group, whereas the band at 1659 cm<sup>-1</sup> is caused by the thiazole ring's C=N stretching mode.

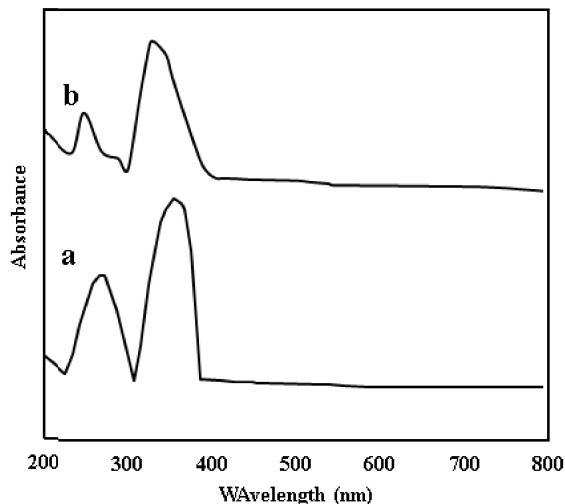


Figure 2: UV-Visible spectra of (a)BOF-II copolymer, (b)Composite

The composite's FTIR spectra are shown in Fig. 3(b). According to the findings, the spectrum of composites differs slightly from the spectrum of copolymer[28]. The band at 3741 cm<sup>-1</sup> represents the asymmetric and symmetric vibrations of the -NH group created by copolymers. This clearly illustrates composites creation. Furthermore, a band at 1478 cm<sup>-1</sup> is caused by the -NO<sub>2</sub> group stretching mode of the benzothiazole ring. The -C=N stretching of the thiazole ring results in a band at 1653 cm<sup>-1</sup>. The band at 2949cm<sup>-1</sup> is created by the aromatic ring's -CH stretching vibrations. Because of the C=O stretching vibration, a band developed at 1588 cm<sup>-1</sup>.The band that formed at 3204cm<sup>-1</sup> causes the -CH<sub>2</sub> asymmetric and symmetric vibrations in the copolymers. The appearance of a 1473cm<sup>-1</sup> absorption band verifies the presence of a -CH<sub>2</sub> bending vibration in the N-CH<sub>2</sub>-N bridge. The 2,6,8-tri substituted benzothiazole ring forms distinct, medium/weak absorption bands from 1306-934 cm<sup>-1</sup>. The presence of the C-S-C group is confirmed by the band at 860cm<sup>-1</sup>. The copolymers interact with the charcoal because the observed bands differ. Under the given conditions, the copolymers and activated charcoal composites were successfully synthesized.

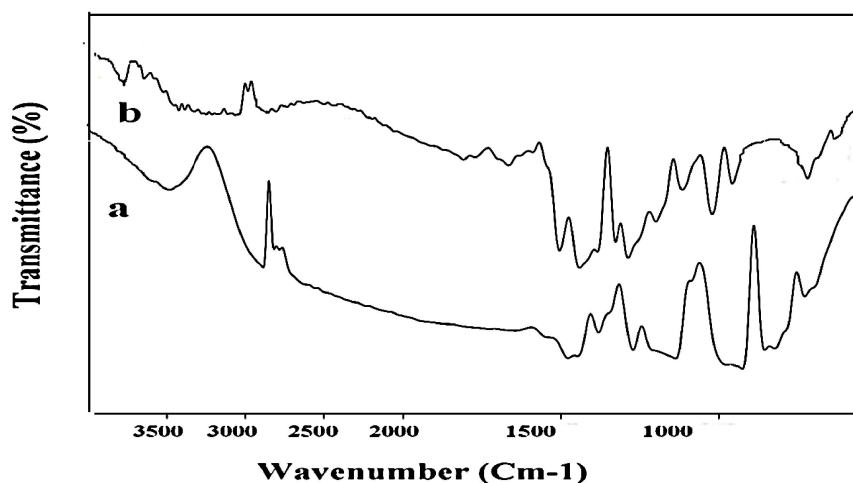
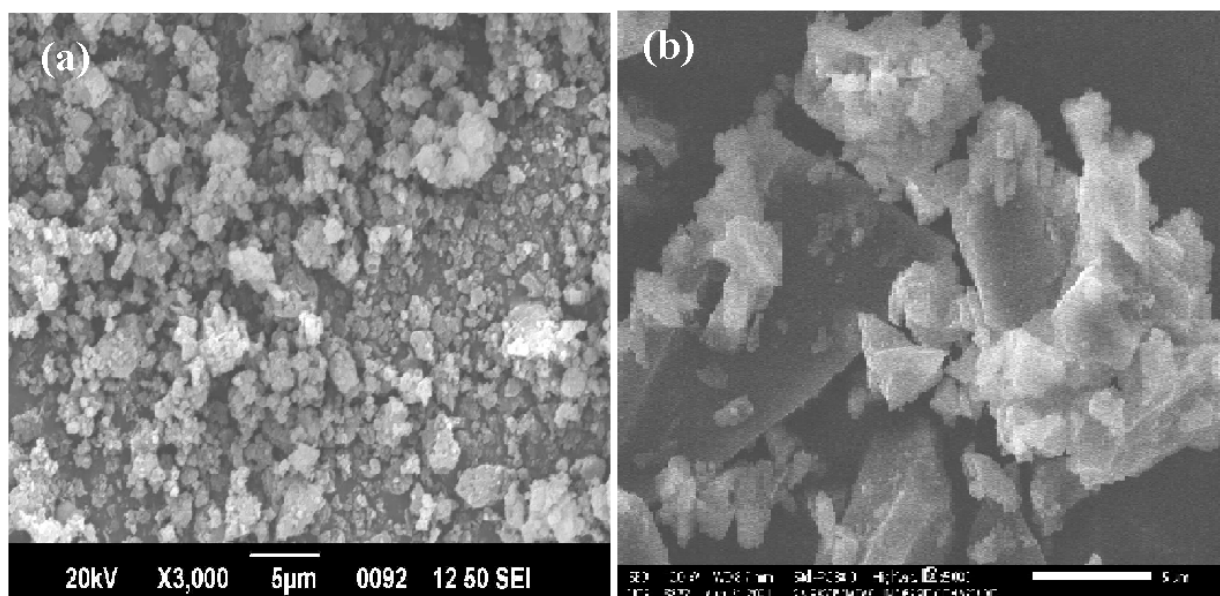


Figure 3: FTIR spectra of (a) BOF-II copolymer, (b) Composite

### 3.4 Surface Analysis

Scanning electron micrographs at various magnifications were used to analyze the morphology of the BOF-II copolymer and its composite with activated charcoal, as shown in Fig. 4, with the white bar at the bottom of the micrographs showing the scale. It describes the structure's surface topography and defects. The BOF-II copolymer has a closely packed structure with deep pits and more active sites, similar to irregular granular particles which are shown in Fig. 4(a). The copolymer is porous, and SEM photographs of the surface morphology of the BOF-II copolymer revealed a fringed representation of the semicrystalline structure. The fringes in the micrographs indicate that the copolymer is transitioning between amorphous and crystalline states. The acidic nature of a monomer determines its degree of crystalline characteristic. Polymerization converts the crystalline structure of the monomer into the amorphous phase of the copolymer. Some noticeable holes and cracks may result from air voids. Fig. 4(b) shows SEM images of the composite. When compared to copolymer, the surface morphology of the composite exhibits an excess of active sites and distinct pores. This implies that increasing the surface area of the composite resulted in the formation of more cavities. The photos demonstrate that the synthesized copolymer and activated charcoal, which has a greater surface area and more active sites, formed very firmly in the composite.



**Figure 4:** SEM images of (a) BOF-II copolymer, (b) Composite

### 3.5 Thermal Degradation Studies

The thermogravimetric analysis was used to assess the kinetics of deterioration as well as the change in thermal stability of copolymer and composite with the use of thermodynamic parameters. Fig. 5 depicts the TG curves for copolymer and composite. Table 2 shows the copolymer and composite thermal deterioration data. Fig. 5(a) displays three stages of degradation response for BOF-II copolymer from 120–380°C, 380–520°C, and 520–800°C. After the loss of a water molecule in the temperature range 40–800°C, the first disintegration occurs between 40–120°C, compared to 3.02% computed, which may be attributed to the loss of a water molecule against the determined 3.29% present per repeat unit of the polymer. The loss of the benzothiazole ring may be the cause of the main stage deterioration between 120–380°C (noticed 68.45% and determined 67.97%). The second step of disintegration commences around 380–520°C, resulting in an 80.86% loss of disposal of basic molecules such as –NH and –CH<sub>2</sub> groups contained in the copolymer vs a determined 81.68. The third stage begins at 520–800°C, confirming the oxamide moiety deprivation from the copolymer (99.18% noticed and 100% determined). Copolymer has a half decomposition temperature of 340°C. Fig. 5(b) depicts the composite's thermal degradation curve, and Table 2 summarizes the observed results. With a three-stage pattern, the decomposition temperature varies from 40°C to 1000°C. A deterioration was seen in the initial (first)



stage at 160 °C, which is attributable to the removal of water molecules (moisture). The observed decomposition between 160°C and 520°C relates to second stage degradation, which could be related to the elimination polymeric matrix. Finally, the third step breakdown runs from 520°C to 1000°C, corresponding to the remaining carbonized charcoal, confirming the creation of polymeric composite. According to the TGA data, the composite has more thermal stability than the copolymer that was strongly associated with charcoal.

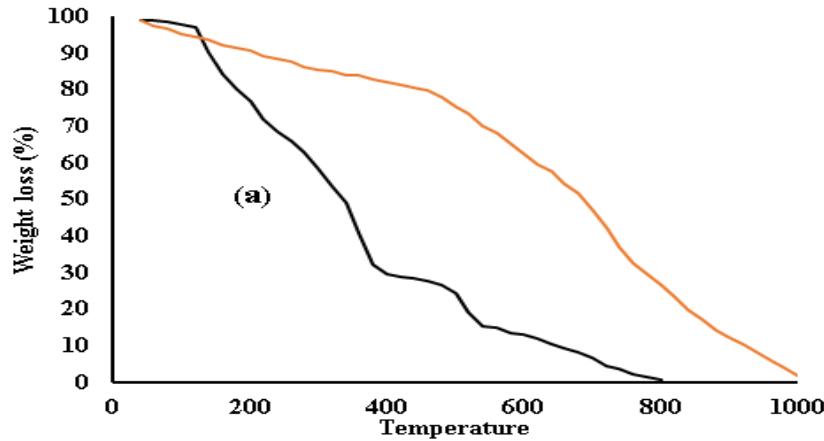


Figure 5: Thermograms of BOF-II copolymer and its composite

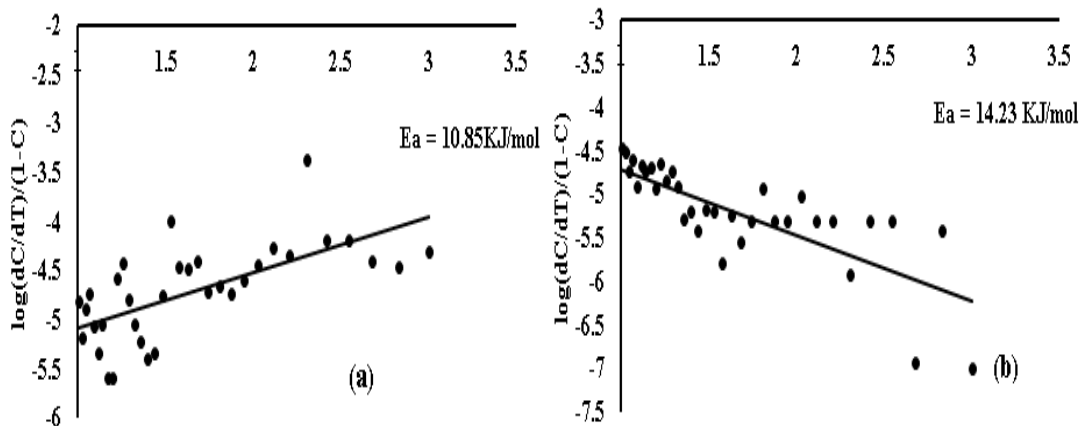


Figure 6: Sharp-Wentworth plot (Ea) for (a) BOF-II copolymer (b) Composite

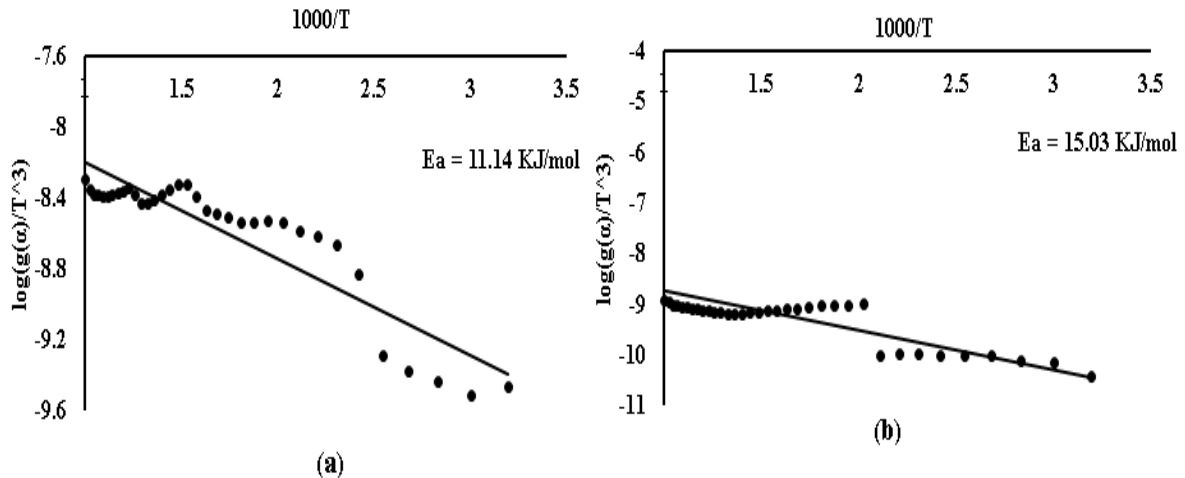


Figure 7: Freeman-Carroll plot (Ea) for (a) BOF-II copolymer (b) Composite

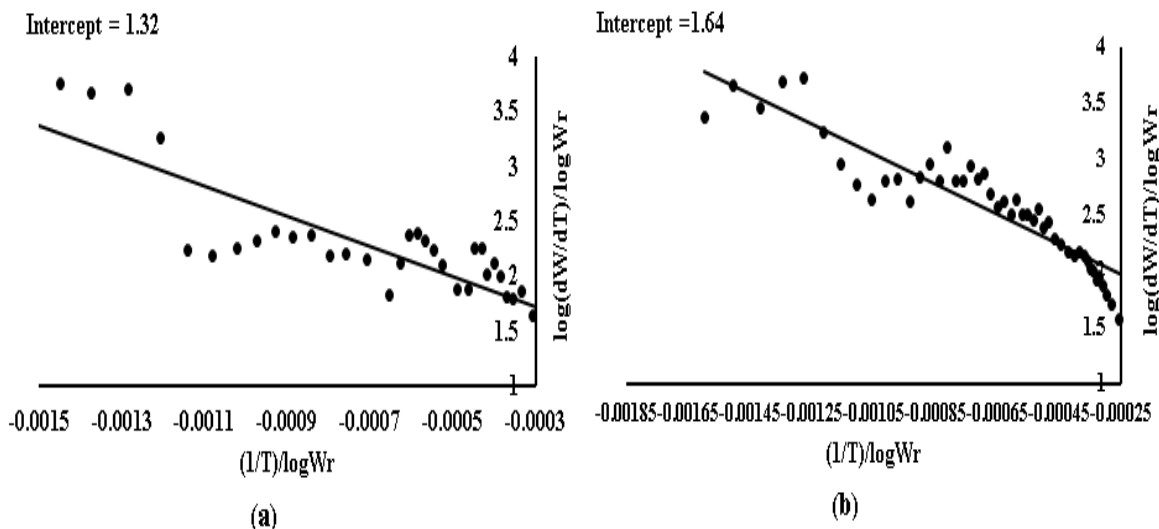


Figure 8: Freeman-Carroll plot (n) for (a) BOF-II copolymer (b) Composite

3.6 Kinetics of Thermal Degradation

Sharp-Wentworth and Freeman Carroll techniques are used to derive thermodynamic parameters ( $\Delta S$ ,  $\Delta F$ ,  $Z$ ,  $S^*$ ) which can be estimated based on thermal activation energy ( $E_a$ ) using equations (3), (4), (6), and (7) for the copolymer and composite from observed TG data, and the results are shown in Table 2. Figs. 6 and 7 show that the activation energy computed by Sharp-Wentworth and Freeman-Carroll methods for copolymer and its composite is found to be in good agreement with each other. According to the results, the copolymer and composite would have a larger molecular weight and thermal stability based on the activation energies. As the activation energy increases, thermal stability also gets increased, and therefore from the observed results of TGA, it was clear that the activation energy of the BOF composite was to be high as compared to the copolymer which is due to the rich carbon source in copolymer and its composite. The FC technique revealed that the thermal degradation of BOF-II copolymer and its composite was of the first order which was shown in Fig. 8. During the thermal degradation process, an abnormally low-frequency factor was discovered, which might be attributed to the slow decomposition reaction that happened for copolymer and its composite. The negative entropy change value indicates that the compounds have a more ordered structure than the reactants and that the reaction is slower than expected, as supported by the low-frequency factor ( $Z$ ) value. Based on the information presented above, composites have greater thermal stability than copolymer.

Table 2: Kinetic Parameters of BOF-II copolymer and its composite.

Compound	Activation energy $E_a$ (kJ/mol)		Entropy Change $\Delta S$ (J)	Free Energy Change $\Delta F$ (kJ)	Frequency factor $Z$ ( $S^{-1}$ )	Apparent Entropy Change ( $S^*$ )	Order of reaction (n)
	*SW	*FC					
BOF-II copolymer	10.85	11.14	-192.40	60.78	483.59	-62.89	1.32
BOF composite	14.23	15.03	-198.88	64.23	523.74	-68.26	1.64

\*SW: Sharp-Wentworth and \*FC: Freeman-Carroll

Change of Entropy:

$$\text{Intercept} = [\log KR/h\phi E] + S / 2.303 R \text{ ----- (3)}$$

Where,  $K = 1.3806 \times 10^{-16}$  erg/deg/mole,

$R = 1.987$  Cal/deg/mole

$h = 6.625 \times 10^{-27}$  erg sec,

$$\phi = 0.166$$

S = Change in entropy,

E = Activation energy from graph.

**Free Energy Change:**

$$\Delta F = \Delta H - T\Delta S \text{-----(4)}$$

Where,  $\Delta H$  = Enthalpy Change = activation energy

T = Temperature in K

S = Entropy change from (i) used.

**Frequency Factor:**

$$B_n = \log Z E_a / \phi R \text{----- (5)}$$

$$B_1 = \log [\ln 1 / 1 - \alpha] - \log P(x) \text{----- (6)}$$

Where, Z = frequency factor,

B = calculated from equation (6)

Log P(x) = calculated from Doyle's table corresponding to the activation energy.

**Apparent Entropy Change:**

$$S^* = 2.303 \log Z h / K T^* \text{----- (7)}$$

Z = from relation (5)

T\* = temperature at which half of the compound is decomposed from its total loss.

**III. CONCLUSION**

The BOF-II copolymer was synthesized with good yield by polycondensation polymerization of 2-amino 6-nitobenzothiazole and oxamide with formaldehyde in a 2:1:3 molar ratio, and its composite was prepared by ultrasonication method using activated charcoal in 1:2 ratio. On comparing, FTIR, and UV-Visible spectra of copolymer and its composite shows the shifting of bands which confirms the formation of composites. The surface morphology indicates that the BOF-II copolymer shows a transition state between the crystalline and amorphous phases. Also, the SEM micrograph shows that the composite exhibits an excess of active sites and distinct pores when compared with copolymer which is because of the increased surface area of the composite. From the value of activation energy calculated by Sharp-Wentworth and Freeman-Carroll methods for copolymer and its composite is found to be in good agreement with each other and have high thermal stability. The synthesized copolymer and its composite show slow thermal degradation reaction is explained based on the low values of frequency factor, and from the value of the order of reaction it is clear that copolymer and its composite approximately follow first-order kinetics. Hence, based on TGA data of copolymer and its composite it reveals that the thermal stability of the composite is higher than copolymer, possibly due to more carbonized residues.

**ACKNOWLEDGMENT**

The authors express their gratitude to the STIC, Cochin, SAIF, Punjab University, SAIF, Dharwad University, RUSA Nagpur University, and Kamla Nehru Mahavidyalaya, Nagpur, for completing the sample characterization.

**REFERENCES**

- [1]. C. Wan-yuan, W. Jin-Yin and C., Huaxue Yu Nianhe, 1 (2002) 20–21.
- [2]. A.N. Egorov, Y. I. Sukhorukov, G. V. Plotnikova, and A.K. Khaliullin, Russ. J. Appl. Chem., 75(1) (2002) 152–155.
- [3]. W. B. Gurnule, P. K. Rahangdale, L. J. Paliwal, R. B. Kharat, React. Func. Polym., 55 (3) (2003) 255-265
- [4]. R. N. Singru, A. B. Zade, and W. B. Gurnule, J. Appl. Polym. Sci., 109(2) (2008) 859–868.
- [5]. P. E. P. Michael, J. M. Barbe, H. D. Juneja, and L. J. Paliwal, European Polym. J., 43(12) (2007) 4995–5000.

- [6]. D. K. Raval, B. N. Narola, and A. J. Patel, Iran. Polym. J., 14(9) (2005) 775–784.
- [7]. M. M. Patel, and R. Manavalan, Die Makromolekulare Chemie, 184(4) (2003) 717–723.
- [8]. P. K. Rahangdale, W. B. Gurnule, L. J. Paliwal, and R. B. Kharat, Progr. Cryst. Grow. and Charact. Mater., 45(1-2) (2002) 155–160.
- [9]. M. V. Tarase, A. B. Zade, and W. B. Gurnule, Journal of Ultra Scient. Physic. Sci., 3(1) (2007) 41.
- [10]. M. M. Jadhav, L. J. Paliwal, and N. S. Bhave, J. Appl. Polym. Sci., 101(1) (2006) 227–232.
- [11]. S. P. Chakole, K. A. Nandekar, W. B. Gurnule, J. Phys: Conf Ser. 1913 (2021) 012062.
- [12]. W. B. Gurnule, Y. U. Rathod, Curr Appl Polym Sci 4 (2020) 1-8.
- [13]. Rathod Y., U., Zanje S., B., Gurnule W., B., J. Phys Conf Ser 1913 (2021) 012061
- [14]. S.S. Butoliya, W.B. Gurnule and A.B. Zade, E-J. Chemistry, 7(3) (2010) 101-107.
- [15]. W.B. Gurnule, N.C. Das, S. Vajpai and Y.U. Rathod, Mater. Tod: Proc., 29(4) (2020) 1071-1076.
- [16]. D.T. Masram, N.S. Bhave and K.P. Kariya, J Chem., 7 (2010) 564.
- [17]. R.S. Azarudeen, M.A.S. Ahamad, D. Jeyakumar, A. R. Burkanudeen, Iran. Polym. J., 18(10) (2009) 821-832.
- [18]. J. V. Khobragade, M. Ahamed and W. B. Gurnule, Intern. J. Resear. in Bioscience, Agri. and Tech., (1) (2015) 2347-2366.
- [19]. E.S. Freeman, and B. Carroll, The J. Phys. Chem., 62(4) (1958) 394-397.
- [20]. J. B. Sharp, and S. A. Wentworth, Analytical Chemistry, 41(14) (1969) 2060-2062.
- [21]. R. N. Singru, A. B. Zade, and W.B. Gurnule, J. Appl. Polym. Sci., 109 (2008) 859-868.
- [22]. C.G. Kohad, and W.B. Gurnule, IJCESR, 6(1) (2019) 503-512.
- [23]. W. B. Gurnule, and J. V. Khobragade, IJCESR, 6(1) (2019) 116-122.
- [24]. G. Velmurugan, K. RiazAhamed, Raja SulaimanAzarudeen, and M.Thirumarimurugan, Sep. Sci.Tech., (2017) 1-54.
- [25]. G. Velmurugan, K. RiazAhamed, Raja S. Azarudeen, and M.Thirumarimurugan, Polym. Comp., (2015) 1-41.
- [26]. B.H. Stuart, Infrared Spectroscopy: Fundamentals and Applications, New York: Wiley, (2004).
- [27]. J.M. Thompson, Infrared Spectroscopy, Jenny Stanford Publishing, (2018).
- [28]. W.B. Gurnule, K. Vajpai, and A.D. Belsare, Materials Today: Proceedings, (2020), 1-7, 2020.